Reprint Series
21 May 1982, Volume 216, pp. 805–812

SCIENCE

Ion Beam Spectroscopy of Solids and Surfaces

Barbara J. Garrison and Nicholas Winograd

21 May 1982, Volume 216, Number 4548 SCIENCE

Ion Beam Spectroscopy of Solids and Surfaces

Barbara J. Garrison and Nicholas Winograd

Summary. Ion beams are important new probes for characterizing the chemistry and structure of a wide variety of materials. When beams of particles with energies of ~ 1000 electron volts are used, as in secondary ion mass spectrometry, it is possible to detect ions ejected from the top layer of the material with sensitivities well below the picogram level. A number of theoretical developments now permit analysis of the geometry of adsorbed atoms and molecules on surfaces from the angular distributions of the ejected particles. Much surface chemical information can also be deduced from ejected molecular cluster ions. In addition, the observation of clusters with weights up to nearly 20,000 atomic mass units promises to expand applications of mass spectrometry to the analysis of biomolecules and the sequencing of proteins.

When a beam of particles is allowed to interact with a solid, the resulting scattering events have the potential to provide a variety of fundamental structural and chemical information. Analysis of this type of scattering may appear somewhat unusual, since it is much more common for spectroscopists to use photons or electrons to characterize the energy states of matter. Particle beams, however, have a number of useful and unique properties that promise to greatly expand their applications during the next decade.

One possible experimental configuration—and the one we focus on in this article—is illustrated in Fig. 1. The sample is represented as a single crystal by an ordered array of spheres containing, in this case, three layers. The atom above the crystal in Fig. 1a represents the incident particle, whose kinetic energy is generally between a few hundred and a few thousand electron volts. After the initial collision, the atoms in the crystal begin to move in various directions as the energy of the incident particle is shared among them. At these energies the trajectories of the particles can be described by using the classical equations of motion since the wavelengths λ of the particles, as calculated by the de Broglie relation $\lambda = h/mv$ (h is Planck's constant and m and v are mass and velocity), are extremely small relative to atomic spacings. The results of such a calculation are shown in Fig. 1b. After less than 10^{-12} second some particles have been ejected into the vacuum and may therefore, in principle, be detected in the laboratory. Note also that there are two atoms being ejected toward the left in Fig. 1b which appear to be stuck together as a diatomic molecule or dimer.

The question is, can we learn something about the solid by a detailed analysis of the motion subsequent to the primary bombardment event? The answer to this question is not obvious. In fact, the difficulty can be illustrated by an analogy from the game of pool. Here, a cue ball is incident upon a triangular array of 15 target spheres placed on an isolated surface. Suppose a player comes into the room with the pool table and then initiates the action. After all the balls stop moving, he leaves the room, and a second observer enters who is asked to reconstruct the original configuration of the balls. He is asked not only to reveal their original structure but also to place the numbered balls in sequence. Thus, was the eight ball originally touching the two ball? If this could be done on an atomic scale, we could obviously learn a great deal about the structure and interaction between atoms near the point of impact of the bombarding particle.

The study of the interaction of energetic particles with solids has been an active field of research since the observation by Grove (*1*) in 1850 that the cathode in a discharge source was easily eroded by gas ions in the tube. The phenomenon was referred to in those days as sputtering, implying that matter is ejected from the areas of the surface that are struck by the bombarding species. More recently, applications of ion beam methods have appeared in such diverse fields as ion implantation, particularly for doping semiconductors, fusion reactor design, determining the effect of wall reactions on plasma temperatures, and modeling the influence of the solar wind (He^+) on extraterrestrial surfaces (*2*). Interest may be focused on the damage to the solid by the incident particle or on the analysis of the ejected material.

The analysis of surface composition with ion beams is based on the fact that a fraction of the ejected particles leave the surface as positive or negative ions. These ions may be detected directly with a mass spectrometer. In this approach, usually referred to as secondary ion mass spectrometry (SIMS), elements with low ionization potentials or high electron affinities (H^+, Na^+, K^+, O^-, Cl^-, Br^-, F^-, and so on) can be determined with detection limits approaching 10^{-14} gram (*3*). In addition, the primary ion can be focused to a diameter of 100 nanometers, allowing high spatial resolution. This ion microprobe configuration has been applied in the fields of catalysis, geology, biology, semiconductor technology, and metallurgy (*4*) to yield element-specific micrographs. A major difficulty in measuring the ions that are created at the surface during the ejection

Barbara Garrison is an assistant professor of chemistry and Nicholas Winograd is a professor of chemistry at The Pennsylvania State University, University Park 16802.

0036-8075/82/0521-0805$01.00/0

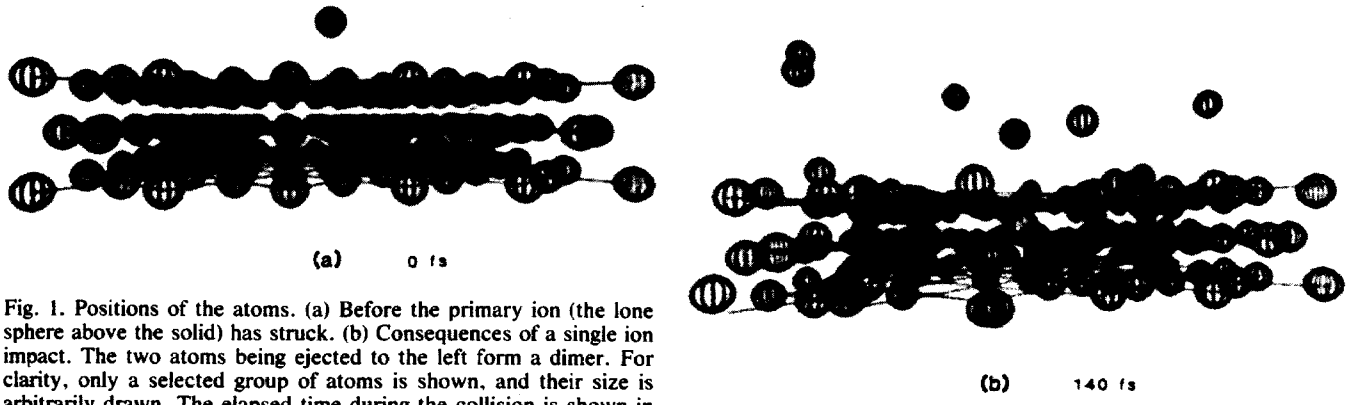

Fig. 1. Positions of the atoms. (a) Before the primary ion (the lone sphere above the solid) has struck. (b) Consequences of a single ion impact. The two atoms being ejected to the left form a dimer. For clarity, only a selected group of atoms is shown, and their size is arbitrarily drawn. The elapsed time during the collision is shown in femtoseconds (1 fs = 10^{-15} second).

process is that the ionization probability, R^+, depends strongly on the electronic properties of the sample. For a given element R^+ has been found to vary over many orders of magnitude, depending on the degree of surface oxidation (*5*). It is possible, although generally with a large loss of sensitivity, to use some sort of post-ionization of the neutral species, which makes the technique much more quantitative (*6*).

As illustrated in Fig. 1, the primary ion creates a great deal of damage near the point of impact, which could alter the chemical nature of the sample. Benninghoven (*3*) pointed out that this effect could be minimized by keeping the total number of primary ions at least an order of magnitude smaller than the total number of surface molecules. In practice, this amounts to exposing the sample to a 10^{-9} ampere beam spread over ~ 1 square centimeter for about 10^2 to 10^3 seconds. In addition,since a wide area is imaged into the mass spectrometer, the sensitivity could be considerably enhanced by using a quadrupole mass filter instead of the conventional magnetic sector normally employed in mass spectrometry. This analyzer also has the advantage of being relatively easy to connect to an ultrahigh vacuum (10^{-10} torr) environment, a necessary condition for the characterization of clean surfaces.

Since this experimental breakthrough, several research groups have recorded the mass spectra of metal surfaces exposed to a number of simple gas molecules. Model systems have included CO, O_2, and H_2 on Ni (*5*, *7*), O_2 and CO on Mo (*8*), and O_2 on W (*9*). The resulting ion yields reflect the coverage and chemical state of the adsorbed molecules. For example, molecularly adsorbed CO can be distinguished from dissociatively adsorbed CO on Ni by the presence of an $NiCO^+$ cluster ion (*7*). A number of other molecules, including amino acids (*10*), organometallic compounds (*11*), alkali halides (*12*), and even proteins (*13*), have been found to be ejected intact from bombarded metal surfaces. In addition, the angular distributions of ions ejected from single crystals have been found to be highly anisotropic (*14*) and indicative of the surface symmetry; this observation opens the door to determining geometric properties of adsorbed layers, a fundamental problem in surface science.

In this article, we examine theoretical developments that have led to an understanding of some of the observations mentioned above, and outline several new applications of ion beams for characterizing solids and surfaces. We focus on the SIMS experiment, where ejected atomic and molecular cluster ions are detected. We ignore the fate of the incident particle, even though it has been the subject of some interesting experiments; for example, the techniques of ion scattering spectrometry, MeV backscattering, and atomic beam diffraction are yielding detailed information about the structure of solid surfaces (*15*).

Dynamics of the Scattering Events

Although a great deal of spectral data can be generated by scattering ion beams from surfaces, it is another matter to understand such a complex process. One approach, which has proved to be quite successful in elucidating the nature of the momentum dissipation, is to employ classical dynamics to compute the positions and momenta of all the relevant particles as a function of time after impact of the primary ion. This technique has been successful in examining atom-diatom scattering, properties of liquids, and even the solvation of large molecules such as dipeptides (*16*). It was first applied to ion impact phenomena by Gibson *et al.* (*17*) with alkali halide substrates and later by Gay and Harrison (*18*) with copper microcrystallites. More recently, computers have been used to extend these early qualitative studies and provide at least semiquantitative predictions of the particle ejection process.

The theoretical model begins with a microcrystallite that is four or five atomic layers deep and contains 60 to 100 atoms per layer (*19*). The motion of all the atoms is computed by numerically integrating Newton's equation, force = mass × acceleration. In practice, between 100 and 1000 trajectories or primary ion hits are computed at impact points over an irreducible surface symmetry zone to obtain the macroscopic yield of particles and other observables. The calculation during a single ion trajectory is stopped after it is energetically impossible for the fastest moving atom to be ejected. Ideally, the size of the model microcrystallite is selected so that further size increases do not change the observable of interest. From the final positions and momenta of the particles above the surface, the yield (number of particles ejected per incident particle), ejection energies, and angles can be determined. By analyzing for interactions between ejected atoms, it is also possible to check for the possibility of cluster formation. The model is quite general in that different crystal structures or faces can be set up. Chemisorbed atoms or molecules can be placed in arbitrary locations and coverages on the microcrystallite surface. The procedure has been described in detail in many articles (*19*–*21*).

Although the classical dynamical procedure is an extremely powerful one, there are two difficulties that prevent a complete solution to the problem. First, in order to calculate the forces between the atoms, one must know the interaction potential surface for all the atoms in the microcrystallite. Considerable effort has been expanded to find the correct

potentials, and although certain forms have gained popularity, it is not clear that any are accurate. One approach is to construct a pairwise additive function from an exponential repulsion at small internuclear separations and a long-range attractive Morse potential (*20, 22*). The calculations are then restricted to cases where the choice of potential parameters is not particularly important. The angular distribution of particles ejected from single-crystal surfaces represents such a case (*23*). The calculation of yields, on the other hand, is very sensitive to the chosen depth of the Morse potential well (*24*).

The second difficulty is that the ionization process needs to be included in the model, since electronic motion is ignored in the classical calculations. However, the theory of the ionization process has been a subject of intense debate over the past decade. The difficulty began when it was observed that there was an empirical correlation between log R^+ and the difference between the ionization potential (or electron affinity for negative ions) and the surface work function (IP − Φ) for a number of elements (*25*). This observation was confirmed quantitatively by Yu (*26*), who measured log R^+ and Φ simultaneously during deposition of submonolayers of Cs on Mo. The result was first interpreted by Andersen and Hinthorne (*25*) in terms of a local thermal equilibrium (LTE) model, which treated the region about the impact point as a high-temperature plasma of ions, electrons, and neutral species. Although the resulting equation has the correct form, it has not been possible to see the physical significance of such a model, especially after examining Fig. 1. The classical dynamical calculations clearly show that only a few collisions lead to particle ejection and that there is nothing approaching a thermal environment in this region.

A more satisfying quantum mechanical approach is under development. In this model the electronic levels of the ejecting atom are allowed to mix with the manifold of states within the solid. The value of R^+ is then determined by solving the time-dependent Schrödinger equation, using an appropriate coupling interaction between the leaving species and the solid. Blandin *et al.* (*27*) and Norskov and Lundqvist (*28*) have generalized this model by assuming a continuum of levels in the solid and allowing for the tunneling of electrons from occupied states below the Fermi level. The expression for R^+ is

$$R^+ = 2/\pi\{\exp[-C_1\pi(\mathrm{IP} - \Phi)/\hbar\lambda v]\} \quad (1)$$

where $\hbar$ is Planck's constant divided by 2π, λ is a coupling parameter, v is the particle velocity, and C_1 is a constant and is of the same form as suggested by the LTE model.

In a major advance, Sroubek *et al.* (*29*) have developed a similar model that allows for nuclear motion within the solid. Although their model is similar to that described above, they find a much weaker dependence of R^+ on velocity. This prediction has been tested in two recent experiments. Yu (*30*) found that for TiO_2 substrates the velocity dependence of R^+ followed Eq. 1 at oxygen ion energies greater than ~ 15 eV, but that R^+ was nearly independent of velocity at very low kinetic energies. Gibbs *et al.* (*31*) measured the polar angle distributions of Ni^+ ejected from a CO-covered Ni surface and found good agreement with classical dynamical calculations if a simple image force correction is included. This force is expected to influence ions near metal surfaces due to the polarization of the metallic electrons. The observation implies that R^+ is only weakly dependent on kinetic energy. Thus it appears that neglect of ionization processes in the classical dynamical calculations should not be a serious problem when attempting to describe the basic ejection mechanisms of the ions observed in SIMS.

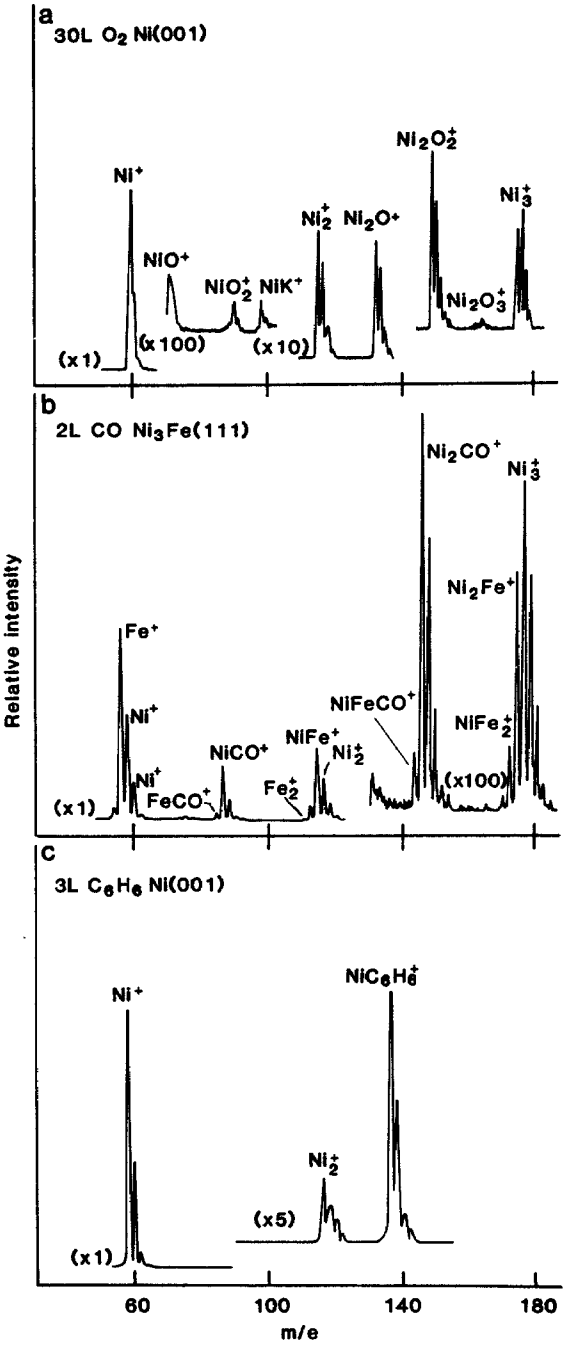

Fig. 2. Typical cluster ions observed by SIMS. (a) Positive ion spectrum for Ni(001) exposed to 30 langmuirs (1 L = 10^{-6} torr) of oxygen. (b) Positive ion spectrum for $Ni_3Fe(111)$ exposed to 2 L of CO. (c) Positive ion spectrum for Ni(001) exposed to 5 L of benzene.

Molecular Clusters and How They Form

The combination of ion bombardment experiments on well-defined single crystals and the results of classical dynamical calculations provides a sound basis for examining many fundamental aspects of ion beam methods. An important property of these methods involves the fact that molecular cluster species are often ejected from the surface. For adsorbates on clean metals these vary from pure metal clusters M_n, where n can be 12 or more (*32*), to metal atoms attached to adsorbed species, such as NiO and NiCO (*5*, *7*), and to large organic molecules which were originally adsorbed on the surface of the solid and are ejected retaining their molecular formula (*10–12*). Some examples of these spectra are shown in Fig. 2.

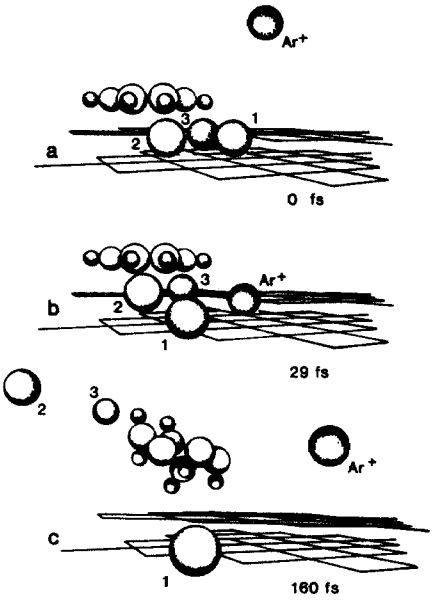

Fig. 3. Ejection of a C_6H_6 molecule by simultaneous collision with two Ni atoms. Only the species [one Ar^+ ion, three Ni atoms (labeled 1, 2, and 3), and one C_6H_6 molecule] directly involved in the collision are shown. Grid lines are drawn between nearest neighbors in each plane; thus a Ni atom is initially situated at each intersection of lines. The sizes of the atoms are arbitrary. (a) Initial positions of the atoms; the benzene is viewed from the side. (b) Positions as the two Ni atoms are about to collide with benzene. (c) Distortion of the ejected benzene. [From (*36*); reprinted with permission from the American Chemical Society]

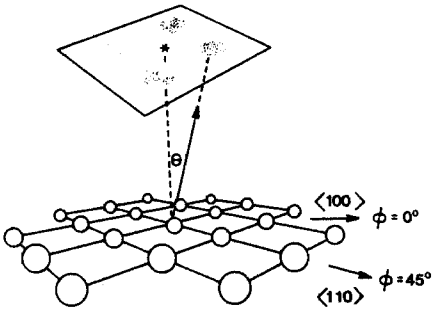

Fig. 4. Schematic representation of the angular distributions of ejected atoms from the (001) crystal face of a face-centered cubic metal. The polar angle is θ and the azimuthal angle ϕ. Note that ϕ = 45° corresponds to the close-packed row of surface atoms.

It has been intriguing to speculate about the origin of these clusters. If they arise from contiguous surface atoms, their presence could provide information about the local atomic structure of complex surfaces such as alloys and supported metal catalysts. They may also yield information about surface bonding geometries. For example, it is of interest to know whether the Ni_2CO^+ cluster originates from a bridge-bonded CO complex on Ni and the $NiCO^+$ cluster arises from a singly or linearly bonded Ni–CO complex (*7*), or whether rearrangement distorts such interpretations.

From the classical dynamical treatment, it is possible to examine the cluster formation mechanism in detail and to provide semiquantitative information about cluster yields. In general, these calculations suggest that there are three basic mechanisms of cluster formation (*33*). First, for clean metals or metals covered with atomic adsorbates, the ejected atoms can interact with each other in the near-surface region above the crystal to form a cluster by a recombination type of process (*20*, *21*, *34*). This description would apply to clusters of the type M_nO_m observed in many types of SIMS experiments and illustrated in Fig. 2a. In this case the atoms in the cluster do not need to arise from contiguous sites on the surface, although in the absence of long-range ionic forces the calculations indicate that most of them originate from a circular region of radius ~ 5 angstroms. This rearrangement, however, complicates any straightforward deduction of the surface structure from the composition of the observed clusters. A second type of cluster emission involves molecular adsorbates such as CO on Ni_3Fe, as shown in Fig. 2b. Here, the CO bond strength is ~ 11 eV, but the interaction with the surface is only about 1 to 2 eV. Calculations indicate (*35*) that this energy difference is sufficient to allow ejection of CO molecules, although ~ 15 percent of them can be dissociated by the ion beam or by energetic metal atoms. For such molecular systems it is easy to infer the original atomic configurations of the molecule and to determine the surface chemical state. If CO were dissociated into oxygen and carbon atoms, for example, the calculations suggest that the amount of CO observed should drop dramatically. The final mechanism for cluster ejection is essentially a hybrid mechanism between the first two. In the case of CO on Ni_3Fe, we find that the observed NiCO, Ni_2CO, and NiFeCO clusters form by a recombination of ejected Ni and Fe atoms with ejected CO molecules. There is apparently no direct relation between these moieties and linear and bridge-bond surface states.

Other, much larger clusters have also been found to be ejected from metal substrates coated with higher molecular weight organic molecules. A SIMS spectrum of benzene adsorbed on Ni(001) is shown in Fig. 2c. Is it possible that the energetic collision cascades produced by a 1000-eV Ar^+ ion can lift a molecule of this size (or larger) from the surface

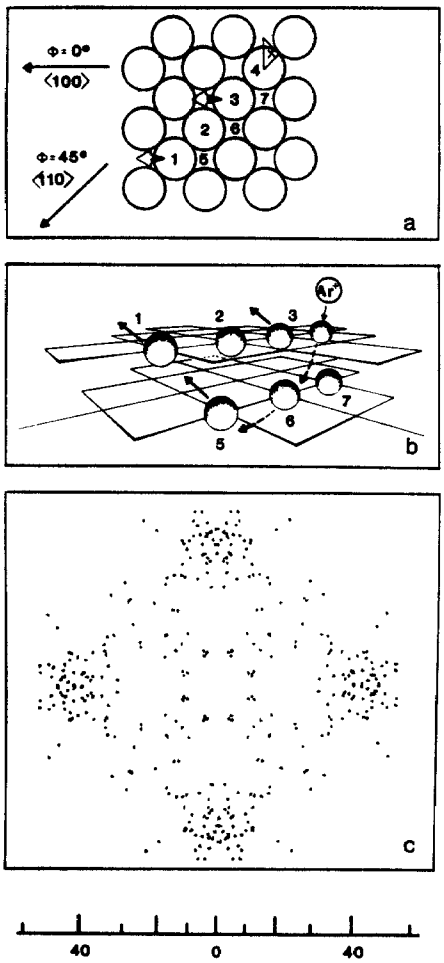

Fig. 5. Mechanism of formation of the Ni_2 dimer, which is preferentially ejected in the <100> directions, contributing most of the intensity to the spot in the angular distribution. (a) Ni(001), showing the surface arrangements of atoms. The numbers are labels and X denotes the Ar^+ ion impact point for the mechanism in (b). (b) Three-dimensional representation of an Ni_2 dimer formation process. For clarity, only the atoms directly involved in the mechanism are shown. (c) Calculated angular distributions of Ni_2 with kinetic energies > 10 eV.

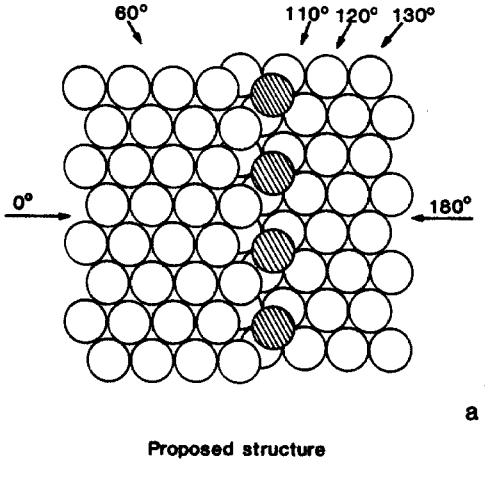

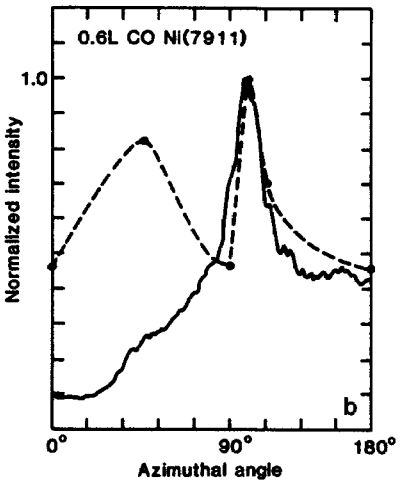

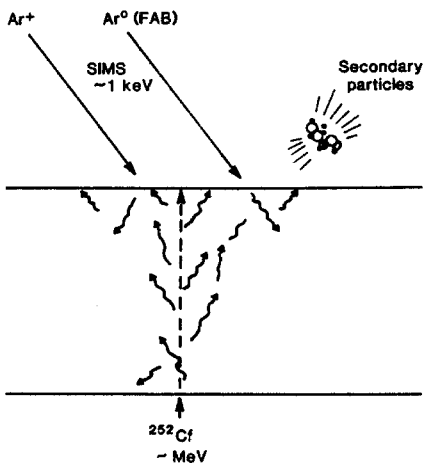

Fig. 6 (left). Ni(7 9 11) with adsorbed CO. (a) Proposed structure. The numbers refer to the incident azimuthal angle of the primary ion. [From (*39*); reprinted with permission from North-Holland Publishing Company] (b) $NiCO^+$ intensity versus azimuthal angle of the bombarding Ar^+ ion. The nickel surface was exposed to 0.6 L of CO. The solid line represents the experimental data and the dashed line results from the classical dynamical calculation. The additional peak at $\phi = 60°$ is not yet understood. Fig. 7 (right). Schematic representation of desorption due to the initiation of energetic collision cascades.

intact? According to classical calculations (*36*) it can, partly because the strong carbon framework can take up excess energy from violent collisions. In fact, the most abundant molecular species in the calculation is C_6H_6. The NiC_6H_6 species forms by recombination of an ejected Ni atom with an ejected C_6H_6 molecule. In the experiment only $NiC_6H_6^+$ is observed, presumably because $C_6H_6^+$ is relatively hard to produce while $NiC_6H_6^+$ is readily formed by a reaction of the type

$$Ni^+ + C_6H_6 \xrightarrow[\text{surface}]{} NiC_6H_6^+ \qquad (2)$$

A typical collision sequence leading to benzene ejection is shown in Fig. 3. Other cationized molecules have been observed which are much larger than benzene (*11*, *12*), and we presume that they form by a similar mechanism.

The fact that the composition of the ejected clusters may be different from the original arrangement of surface atoms is somewhat discouraging. As it turns out, however, there are situations where the precise nature of the rearrangement can be predicted theoretically. One example involves the measured O_2^-/O^- ratio as a function of oxygen coverage on Ni(001). This ratio is four times higher for 50 percent oxygen coverage [c(2 × 2) surface] than for 25 percent oxygen coverage [p(2 × 2) surface], a change that is also calculated with the model (*37*). The reason for this effect is that there are no closely neighboring oxygen atoms on the p(2 × 2) surface, and the O_2 formation probability is much lower. Concepts of this sort may be useful in testing for island-growth mechanisms and distinguishing them from those that proceed through several distinct phases. The angular distributions of the molecular clusters may also provide insight into the rearrangement problem, as we shall see next.

Angle-Resolved SIMS and Geometry Determinations

In efforts to determine the geometric arrangements of atoms in and on a surface, ion beams often provide direct information concerning atomic placement. Most of the data can be easily interpreted by classical pictures without relying on quantum mechanics. For example, the directions of the open channels in a crystal can be determined by bombarding with ions with energies of millions of electron volts. By varying the angle of incidence of the beam, the channel direction is found when the ions pass through the solid (*15*). Alternatively, one can detect ions that are reflected from a surface by using ions with energies of about 10 kiloelectron volts (*15*). As the angle of the ion beam approaches grazing incidence, there will be an angle where the reflected ion is no longer detected because an atom on the surface has blocked the exit direction. The angle at which this shadowing occurs is related to the height of the atom on the surface and the magnitude of scattering cross sections.

It is also of interest to ask whether the surface structure will influence the angular distributions of the ejected material during the process illustrated in Fig. 1b. These angular distributions may be displayed by using the scheme illustrated in Fig. 4, where a (001) face is given as an example. Here, each atom's ultimate fate is plotted as a point on a plate high above the solid. Atoms that are ejected perpendicular to the surface ($\theta = 0°$) are plotted in the center of the plate. Note that most particles are ejected along $\phi = 0°$, since there are no atoms in the surface to block their path. The nearest neighbor atom along $\phi = 45°$ inhibits ejection in this direction.

A similar geometric analysis can be made to predict the ejection angles of chemisorbed atoms, for example, oxygen adsorbed on the (001) face of Cu. The oxygen atom should be ejected in the $\phi = 0°$ direction if it is originally bonded above a copper atom, because it is directly in the path of the ejected substrate species. However, if the oxygen is in a hole site, bonded to four substrate atoms, its predicted angle of ejection is $\phi = 45°$ (*23*, *24*). Experiments have confirmed that oxygen resides in a fourfold bridge site because it is ejected in the $\phi = 45°$ direction (*14*).

More surprising than the fact that the directions of the ejected atoms are controlled by the surface structure is the fact that the clusters also exhibit strong angular anisotropies. Figure 5c shows the calculated angular distribution of Ni_2 dimers ejected from a (001) face of nickel. The mechanisms that give rise to the intense region in the Ni_2 distribution at a polar angle of 45° can be ascertained from the dynamical calculations. Most of the dimers that contribute to the spot in the distribution of Fig. 5c are found to arise from similar mechanisms. This is shown schematically in Fig. 5, a and b. The Ar^+ ion strikes target surface atom 4, initiating motion in the solid that eventually ejects atoms 1 and 3 into the

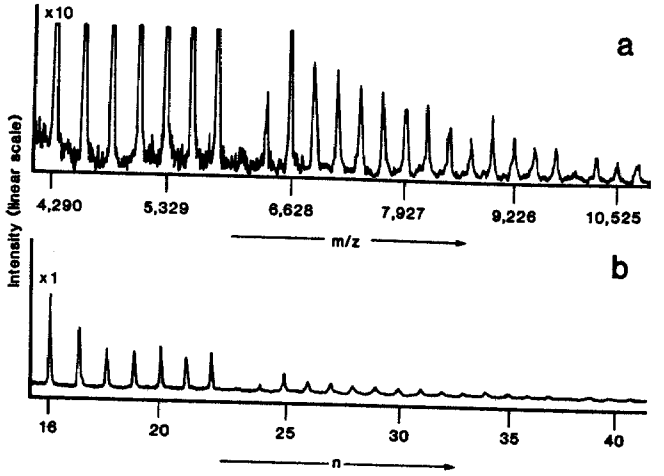

Fig. 8. SIMS spectrum of CsI. [From (*12*); reprinted with permission from the American Chemical Society]

vacuum. Both of these atoms are channeled through the fourfold holes in the $\phi = 0°$ direction, are moving parallel to each other, and are fairly close together. Note that the two atoms that form the dimer do not originate from nearest neighbor sites on the surface. The predictions of these calculations have been confirmed experimentally (*38*).

There is an important ramification of the concept that the dimers that give rise to the maxima in the angular distribution are formed primarily from constituent atoms whose original relative location on the surface is known. If this result were extrapolated to alloy surfaces such as $Ni_3Fe(111)$, the relative placement of the alloy components on the surface would be determined. For example, for the $Ni_3Fe(111)$ spectra in Fig. 2b, there should be no nearest neighbor Fe atoms on a perfect (111) alloy surface, yet an Fe_2^+ peak is observed.

Instead of varying the angle of collection of the ejected particles, it is often fruitful to vary the angle of incidence of the primary ion beam. An interesting system is the stepped Ni(7 9 11) surface, where the steps are five atomic rows wide and one row high. Carbon monoxide at low coverages is believed to preferentially bind in the sites near the lower step edge, as shown in Fig. 6a (*39*). We fix the incident ion beam at a polar angle of 45° and vary the azimuthal angle from 0° to 180°. For virtually all the ions detected, both atomic and cluster species, bombardment down the step, 0° azimuth, causes fewer particles to be ejected than bombardment up the step, 180° azimuth, where the ion can peel off the atoms. The $NiCO^+$ ion intensity is anomalous in that it exhibits a sharp peak at an angle of ~ 120° (Fig. 6b). The dynamical calculations also produce a peak in the NiCO yield at this angle, giving credibility to the proposed structure. Apparently, both the Ni and CO species are channeled from the surface into a small angular cone, favoring cluster formation (*40*). Even though the interpretation is not complete, it is clear that the arrangement of surface atoms controls the nature of the ejection process.

Molecular SIMS and Related Methods

In addition to studying these structural effects, it is possible to use SIMS to detect molecular ions that are characteristic of the original sample. This approach has important implications in chemical analysis and offers a complementary mass spectrometric method for vaporizing and ionizing nonvolatile or thermally unstable compounds. For example, in traditional mass spectrometry, a molecule is usually volatilized by heating and ionized by electron impact. With molecules like amino acids and small peptides, however, heating usually leads to thermal decomposition, whereas ion bombardment may directly produce the desired molecular ion. The subpicosecond time scale of the ion impact event is too fast to allow thermal rearrangements, which occur on a time scale of nanoseconds.

Two other approaches with similar fundamental origins are currently under development. Macfarlane and co-workers (*41*, *42*) discovered that when a thin Mylar foil is bombarded from the back with the fission products of a ^{252}Cf nucleus, molecular ions are ejected from the front of the foil. This technique has been referred to as plasma desorption mass spectrometry and is compared with SIMS schematically in Fig. 7. We believe that the general mechanisms of cluster formation discussed earlier are applicable in this method as well. Although the bombardment energy is in the range of millions of electron volts and energy loss processes are almost certainly electronic in nature, any subsequent collision cascade emanating from the fission track would lead to the ejection of clusters in a fashion nearly identical to that of SIMS.

Another approach has been to employ an atom beam rather than an ion beam as the bombarding species (*13*). The technique has been termed FAB, or fast atom bombardment, rather than SIMS, although the processes are completely identical physically and it is not clear why two names are needed (see Fig. 7). On the other hand, the FAB source offers two unique practical advantages that promise to extend the SIMS applications. First, the secondary ions may be extracted from the sample with a large electrostatic potential without deflecting the primary beam. Second, the proponents of the FAB source suggest that, for insulating samples, charge buildup on the surface is greatly minimized since the incident beam does not alter the sample charge. It is not yet clear that this apparent advantage cannot be offset by the use of standard charge compensation tools such as sample biasing and secondary electron flooding. It is of most interest, however, that these workers have discovered that certain low vapor pressure liquids, such as glycerol, act as ideal solvents for the sample. In this case, the dilution by the matrix apparently minimizes recombination and serves to bring a continually fresh surface to the incident beam, virtually eliminating any sample damage problems.

The analysis of molecular solids by SIMS dates to the early investigations of Benninghoven (*3*) on metal surfaces covered with rather ill-defined organic overlayers. From these observations, he and his co-workers found that even for very delicate organic molecules such as amino acids, ion-bombarded powders of the sample could produce very well defined spectra (*10*). For example, for cysteine deposited on a silver foil, they found that the main features of the spectra are the presence of the molecular ion peaks at $(M + 1)^+$ and at $(M - 1)^-$ and a rather simple fragmentation pattern associated with the lower mass ranges. The ultimate sensitivity of the method is $< 10^{-12}$ g, making SIMS a potentially very sensitive tool. Cysteine is a particularly good example since it is one of the more thermally labile amino acids.

There are many intricacies associated with the preparation of the sample and the bombardment conditions which have yet to be fully determined. For example, even though intense molecular ion spectra are obtained for benzene adsorbed on

Ni, as shown in Fig. 2c, spectra of solid benzene are characterized by a series of hydrocarbon clusters of stoichiometry C_nH_x, where n = 1 to 30 and x is on the order of n for $n < 10$ and on the order of $n/2$ for $n > 10$ (*43*). The spectra are clearly dominated by recombination of ejecting subunits, making identification of benzene itself nearly impossible. Similar conclusions have been reached by Jonkman and Michl (*44*), who used a liquid He crystal to trap the organic molecule in solid argon in an attempt to simplify the spectra. For solid CH_4, they found hydrocarbon fragments to masses assigned to $C_4H_7^+$ and higher. When CH_4 was diluted in an argon matrix (1:500) at 15 K, CH_4^+ was the species with the highest molecular weight observed (*4*).

From reactions of the type given in Eq. 2, it is obvious that the neutral molecule can be converted into an ion by recombination reactions. Grade *et al.* (*45*) have taken advantage of this idea by mixing large quantities of metal ions such as Li^+ and K^+ into the sample, which results in intense peaks representing cationized molecules. These workers also found that *p*-aminobenzoic acid prepared as a film on Ag foil formed the argentated molecular ion $(Ag + M)^+$, as found for benzene on Ni(001).

The situation becomes more complex when the particles forming the cluster possess long-range attractive forces. For the alkali halides, MA, clusters of the type $(MA)_nM^+$ and $(MA)_nA^-$ are the most commonly observed species, with n having values greater than 20 (*12*). This situation is illustrated in Fig. 8 for the positive ion spectrum of CsI. Presumably, these clusters form by recombination of an M^+ and an A^- over the surface, a very favorable process due to the infinite range of the interaction. The MA molecule can then be sequentially cationized or anionized over the surface of the crystal to build up units contained in the observed cluster ion. Note also that there are certain cluster sizes with unusual intensities. This effect is correlated with the hypothesized dominance of cubic-like clusters having low surface energies (*46*). The peak at n = 13, then, is suggested to represent a rhombohedral shape with the 27 atoms in a 3 by 3 by 3 body-centered cubic structure.

Perhaps the tour de force of molecular SIMS is its ability to detect high molecular weight nonvolatile organic materials—particularly biomolecules. For example, the spectrum of vitamin B_{12} is shown in Fig. 9, with the $(M + H)^+$ ion clearly observable at mass-to-charge ratio (*m/e*) 1355 (*47*). It was recently observed by Barber and co-workers (*13*), using an FAB source, that the protonated molecular ion $(M + H)^+$ of the polypeptide Met-Lys-bradykinin could be desorbed intact and detected at *m/e* 1319. The fragmentation pattern is not hopelessly complex, suggesting that the amino acid sequence could be determined. In fact, Williams and co-workers (*48*) have fully sequenced a protein-derived mixture of a tetradeca- and a pentadecapeptide (molecular weight, 1371) aided by the electron impact sequence determination of only the first four residues from the amino terminus. Complementing these studies, McNeal and Macfarlane (*42*) recently observed a dimer ion of a chemically blocked synthetic deoxydodecanucleotide, using ^{252}Cf desorption at *m/e* 12637. The time is clearly ripe for major applications of these methods to the characterization of large biomolecules.

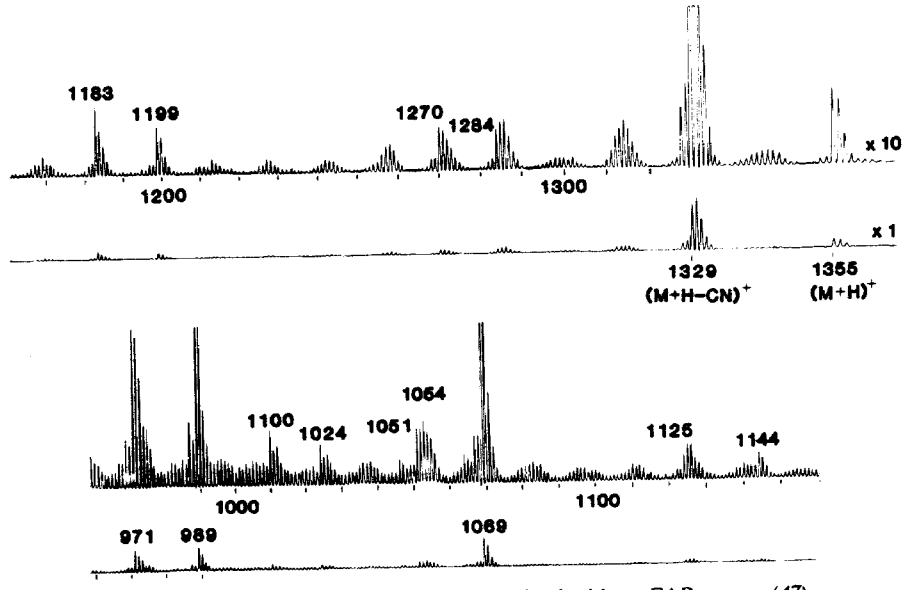

Fig. 9. SIMS spectrum of vitamin B_{12} obtained with an FAB source (*47*).

Conclusions

The applications of ion beam spectroscopy to the characterization of solids and surfaces are rapidly growing. The methods are particularly well suited to examining the local atomic or molecular structure near the point of impact of the primary particle. For example, we have illustrated how angle-resolved measurements can reveal bonding geometries of chemisorbed layers on both flat and stepped surfaces. In addition, the molecular cluster ions are often useful in elucidating the chemistry of the surface. This is particularly true for systems where the rearrangement problem can be minimized, although even this problem can be overcome by using angle-resolved SIMS. Finally, it appears that collision cascades in the solid are capable of desorbing very large molecules without significant decomposition. The prospect of sequencing proteins directly with mass spectrometry is especially exciting.

We believe that the combination of ion bombardment experiments on well-defined single crystals and results from classical dynamical calculations provides a basis for many types of experiments involving particle-surface interactions. These studies should prove invaluable in developing the appropriate theories of cluster formation and in systematically understanding how the SIMS spectra vary with matrix and bombardment conditions. Finally, the atomic trajectories can be followed theoretically on an atomic scale, which is an advantageous feature in the development of ionization models. These models should encompass the characteristics of the atoms located near the particle ejection site.

References and Notes

1. W. R. Grove, *Trans. Faraday Soc.* **142**, 87 (1852).
2. P. K. Haff, C. C. Watson, Y. L. Yung, *J. Geophys. Res.* **86**, 6933 (1981).
3. A. Benninghoven, *Surf. Sci.* **53**, 596 (1975).
4. An excellent review of current applications of SIMS is given in a collection of papers from an international meeting held in Palo Alto, California, on 27 to 31 August 1979 and published in *Springer Series on Chemical Physics*, vol. 9, *Secondary Ion Mass Spectrometry: SIMS II*, A. Benninghoven, C. A. Evans, Jr., R. A. Powell, R. Shimizu, H. A. Storms, Eds. (Springer, New York, 1979).
5. T. Fleisch, N. Winograd, W. N. Delgass, *Surf. Sci.* **78**, 141 (1978).
6. H. Oechsner, W. Ruhe, E. Stumpe, *ibid.* **85**, 289 (1979).
7. H. Hopster and C. R. Brundle, *J. Vac. Sci. Technol.* **16**, 548 (1979); R. S. Bardoli, J. C. Vickerman, J. Wolstenholme, *Surf. Sci.* **85**, 244 (1979); T. Fleisch, G. L. Ott, W. N. Delgass, N. Winograd, *ibid.* **81**, 1 (1979).
8. P. H. Dawson, *Phys. Rev. B.* **15**, 5522 (1977).
9. M. L. Yu, *Surf. Sci.* **71**, 121 (1978).

10. A. Benninghoven, D. Jaspers, W. Sichterman, *Appl. Phys.* **11**, 35 (1976).
11. J. Pierce, K. L. Busch, R. A. Walton, R. G. Cooks, *J. Am. Chem. Soc.* **103**, 2583 (1981).
12. T. M. Barlak, J. R. Wyatt, R. J. Colton, J. J. Decorpo, J. E. Campana, *ibid.*, in press.
13. M. Barber, R. S. Bordoli, R. D. Sedgewick, A. N. Tyler, *J. Chem. Soc. Chem. Commun.* (1981), p. 325.
4. S. P. Holland, B. J. Garrison, N. Winograd, *Phys. Rev. Lett.* **43**, 220 (1979).
15. P. Eisenberger and L. C. Feldman, *Science* **214**, 300 (1981).
16. See, for example, D. G. Truhlar and J. T. Muckerman, in *Atom-Molecule Collision Theory: A Guide for the Experimentalist*, R. B. Bernstein, Ed. (Plenum, New York, 1979), pp. 505–566; P. Lykos, Ed., *ACS Symp. Ser.* **86** (1978); D. J. Rossky and M. Karplus, *J. Am. Chem. Soc.* **101**, 1913 (1979).
17. J. B. Gibson, A. N. Goland, M. Milgram, G. H. Vineyard, *Phys. Rev.* **120**, 1229 (1960).
18. W. L. Gay and D. E. Harrison, Jr., *Phys. Rev. B* **135**, A1780 (1964).
19. D. E. Harrison, Jr., P. W. Kelly, B. J. Garrison, N. Winograd, *Surf. Sci.* **76**, 311 (1978).
20. B. J. Garrison, N. Winograd, D. E. Harrison, Jr., *Phys. Rev. B* **18**, 6000 (1978).
21. ———, *J. Chem. Phys.* **69**, 1440 (1978).
22. D. E. Harrison, Jr., W. L. Moore, Jr., H. T. Holcombe, *Radiat. Eff.* **17**, 167 (1973).
23. N. Winograd, B. J. Garrison, D. E. Harrison, Jr., *Phys. Rev. Lett.* **41**, 1120 (1978).
24. B. J. Garrison, in *Potential Energy Surfaces and Dynamics Calculations for Chemical Reactions and Molecular Energy Transfer*, D. G. Truhlar, Ed. (Plenum, New York, 1981), pp. 843–856.
25. C. A. Andersen and J. R. Hinthorne, *Science* **175**, 853 (1972).
26. M. L. Yu, *Phys. Rev. Lett.* **40**, 574 (1978).
27. A. Blandin, A. Nourtier, D. Hone, *J. Phys. (Paris)* **37**, 369 (1976).
28. J. K. Norskov and B. I. Lundqvist, *Phys. Rev. B* **19**, 5661 (1979).
29. Z. Sroubek, K. Zdansky, J. Zavadil, *Phys. Rev. Lett.* **45**, 580 (1980).
30. M. L. Yu, *ibid.* **47**, 1325 (1981).
31. R. A. Gibbs, S. P. Holland, K. E. Foley, B. J. Garrison, N. Winograd, *Phys. Rev. B*, **24**, 6178 (1981).
32. G. Staudenmaier, *Radiat. Eff.* **13**, 87 (1972).
33. N. Winograd and B. J. Garrison, *Acc. Chem. Res.* **13**, 406 (1980).
34. N. Winograd, D. E. Harrison, Jr., B. J. Garrison, *Surf. Sci.* **78**, 767 (1978).
35. B. J. Garrison, N. Winograd, D. E. Harrison, Jr., *J. Chem. Phys.* **73**, 3473 (1980).
36. B. J. Garrison, *J. Am. Chem. Soc.* **102**, 6553 (1980).
37. N. Winograd, B. J. Garrison, T. Fleisch, W. N. Delgass, D. E. Harrison, Jr., *J. Vac. Sci. Technol.* **16**, 629 (1979).
38. S. P. Holland, B. J. Garrison, N. Winograd, *Phys. Rev. Lett.* **44**, 756 (1980).
39. W. Erley, H. Ibach, S. Lehwald, H. Wagner, *Surf. Sci.* **83**, 585 (1979).
40. K. E. Foley and N. Winograd, to be published.
41. R. D. Macfarlane and D. F. Torgerson, *Science* **191**, 920 (1976).
42. C. J. McNeal and R. D. Macfarlane, *J. Am. Chem. Soc.* **103**, 1609 (1981).
43. G. M. Lancaster, F. Honda, Y. Fukuda, J. W. Rabalais, *ibid.* **101**, 1951 (1979).
44. H. T. Jonkman and J. Michl, *ibid.* **103**, 733 (1981).
45. H. Grade, N. Winograd, R. G. Cooks, *ibid.* **99**, 7725 (1977).
46. J. E. Campana, T. M. Barlak, R. J. Colton, J. J. DeCorpo, J. R. Wyatt, B. I. Dunlap, *Phys. Rev. Lett.* **47**, 1046 (1981).
47. Courtesy of D. J. Surman, Kratos Scientific Instruments.
48. D. H. Williams, C. Bradley, G. Bojesen, S. Santikarn, L. C. E. Taylor, *J. Am. Chem. Soc.* **103**, 5700 (1981); D. H. Williams, G. Bojesen, A. Auffret, L. C. E. Taylor, *FEBS Lett.* **128**, 37 (1981).
49. The financial support of the National Science Foundation, the Office of Naval Research, the Air Force Office of Scientific Research, the Petroleum Research Foundation, the A. P. Sloan Foundation, and the Dreyfus Foundation is gratefully acknowledged.